Proc. Natl. Acad. Sci. USA
Vol. 91, pp. 11655–11659, November 1994
Biochemistry

The secondary structure of the ets domain of human Fli-1 resembles that of the helix–turn–helix DNA-binding motif of the *Escherichia coli* catabolite gene activator protein

HENG LIANG*, EDWARD T. OLEJNICZAK*, XIAOHONG MAO†, DAVID G. NETTESHEIM*, LIPING YU*, CRAIG B. THOMPSON†, AND STEPHEN W. FESIK*‡

*Pharmaceutical Discovery Division, Abbott Laboratories, Abbott Park, IL 60064; and †Howard Hughes Medical Institute and Department of Molecular Genetics and Cell Biology, The University of Chicago, Chicago, IL 60637

Communicated by Alfred G. Redfield, July 28, 1994 (received for review June 9, 1994)

ABSTRACT **The ets family of eukaryotic transcription factors is characterized by a conserved DNA-binding domain of ≈85 amino acids for which the three-dimensional structure is not known. By using multidimensional NMR spectroscopy, we have determined the secondary structure of the ets domain of one member of this gene family, human Fli-1, both in the free form and in a complex with a 16-bp cognate DNA site. The secondary structure of the Fli-1 ets domain consists of three α-helices and a short four-stranded antiparallel β-sheet. This secondary structure arrangement resembles that of the DNA-binding domain of the catabolite gene activator protein of *Escherichia coli*, as well as those of several eukaryotic DNA-binding proteins including histone H5, HNF-3/fork head, and the heat shock transcription factor. Differences in chemical shifts of backbone resonances and amide exchange rates between the DNA-bound and free forms of the Fli-1 ets domain suggest that the third helix is the DNA recognition helix, as in the catabolite gene activator protein and other structurally related proteins. These results suggest that the ets domain is structurally similar to the catabolite gene activator protein family of helix–turn–helix DNA-binding proteins.**

The ets family of transcription factors (1) has been defined by the presence of a conserved region originally identified in the v-*ets* oncogene of the avian retrovirus E26 (2). Members of this gene family are involved in regulating a variety of biological processes including morphogenesis and eye development in *Drosophila* and hematopoietic differentiation in mammals. The deregulation of several *ets* genes by viral transformation or chromosomal translocation has been shown to be oncogenic in humans and other vertebrates (1).

All ets proteins examined to date are sequence-specific DNA-binding proteins that recognize a GGAA/T core flanked by more variable but not random 5′ and 3′ sequences (1). The conserved domain shared by all ets family members is ≈85 amino acids long. This domain, referred to as the ets domain, has been shown by deletion analyses to be principally responsible for the sequence-specific DNA-binding activities of ets proteins (1). Sequence comparisons have not revealed any convincing homologies of the ets domain to other well-characterized DNA-binding motifs such as the zinc finger, homeodomain, leucine zipper, or helix–turn–helix (2). The amino half of the ets domain contains three highly conserved tryptophans that are spaced 17 or 18 residues apart, similar to myb and myb-related proteins (3). The carboxyl portion of the ets domain contains a large number of positively charged residues that cannot be readily aligned with the basic residues of other DNA-binding domains. Patterns of DNA contacts of the ets domain determined from chemical protection studies are not similar to those of the well-characterized classes of DNA-binding proteins and suggest that it binds DNA in a unique manner (4). It is therefore thought that the ets domain may represent a distinct structural motif for DNA binding (2).

Although several predictions have been made of the secondary (5, 6) and the tertiary (7) structures of the ets domain, no experimental data on the structure of ets proteins are available. Here we present the structural characterization of the ets domain of human Fli-1 (8), one member of the ets family. By using heteronuclear multidimensional NMR, we have obtained nearly complete backbone assignments for the Fli-1 ets domain in the unbound form and in a complex with a 16-bp cognate DNA site and have determined the secondary structure of the protein in both forms. In addition, by comparing chemical shifts and amide proton exchange rates in the free and DNA-bound forms, regions of Fli-1 that are involved in DNA binding were identified.

MATERIALS AND METHODS

Protein Expression and Purification. The DNA fragment encoding a 98-amino acid segment (residues 276–373) of human Fli-1 (8, 9) was cloned into pET-3b (Novagen). The bacterially expressed protein, designated Fli-1-(276–373), contains an extra N-terminal methionine. For preparation of uniformly ^{15}N- and $^{15}N/^{13}C$-labeled proteins, transformed cells of *Escherichia coli* BL21(DE3) (Novagen) were grown at 37°C in M9 minimal medium (10) containing appropriate isotopes. Cells for preparing selectively ^{15}N-labeled proteins were grown as described (11).

For purification, cells were resuspended in 20 mM Tricine, pH 8.1/50 mM NaCl/1 mM EDTA/2 mM dithiothreitol (DTT)/1 mM phenylmethylsulfonyl fluoride (buffer I) and lysed by using a French press. $(NH_4)_2SO_4$ was added to the soluble cell lysate to 85%, and the pellet was resuspended in buffer I and dialyzed twice against buffer I. The dialyzed protein suspension was loaded onto an S-Sepharose Fast Flow column (Sigma). Fli-1 was eluted with a gradient of 0.05–0.6 M NaCl in buffer I. After fractions containing Fli-1, as identified by SDS/PAGE, were pooled, the pH was adjusted to 6.5 and $MgCl_2$ was added to 2 mM. This suspension was loaded onto an Affi-Gel Blue column (Bio-Rad) that had been equilibrated with 50 mM NaH_2PO_4, pH 6.5/0.75 M NaCl/2 mM $MgCl_2$/2 mM DTT (buffer II). After washing with buffer II, a linear gradient of buffer II–buffer III (50 mM NaH_2PO_4, pH 6.8/2 M NaCl/1 mM EDTA/2 mM DTT) was

The publication costs of this article were defrayed in part by page charge payment. This article must therefore be hereby marked "*advertisement*" in accordance with 18 U.S.C. §1734 solely to indicate this fact.

Abbreviations: CAP, catabolite gene activator protein; HSQC, heteronuclear single quantum correlation; NOE, nuclear Overhauser effect; NOESY, NOE spectroscopy; DTT, dithiothreitol.

‡To whom reprint requests should be addressed at: Pharmaceutical Discovery Division, Abbott Laboratories, Department 47G, Building AP10, Abbott Park, IL 60064.

applied. Fractions containing Fli-1 were concentrated and exchanged into the NMR buffer (see below). The purified protein was >97% pure, as judged by SDS/PAGE and free of nuclease activities.

Preparation of DNA. The single strands 5′-d(CCCGACCGGAAGTGGG)-3′ and 5′-d(CCCACTTCCGGTCGGG)-3′ were synthesized and purified by HPLC using a Nucleogen-DEAE 60-7 column (Rainin, Woburn, MA) and a gradient of 0.25–0.44 M KCl in 20 mM potassium phosphate/5 M urea, pH 5.5. After desalting on a Sephadex G-25 column, the two strands were mixed at an approximately equal molar ratio and annealed in 10 mM potassium phosphate (pH 7.0). The double-stranded DNA was separated from the single strands over a hydroxyapatite column eluted with a gradient of 10–400 mM potassium phosphate (pH 7.0) and desalted by using a Sephadex G-25 column.

NMR Spectroscopy. NMR samples were in 20 mM Tris-d_{11} maleate-d_4, pH 6.8 (uncorrected for isotope effect)/1 mM EDTA-d_{16}/10 mM DTT-d_{11}/90% H_2O/10% ^2H_2O or 99.9% ^2H_2O. All deuterated reagents were purchased from Cambridge Isotope Laboratories (Andover, MA). NMR data were recorded at 25°C for the unbound form and at 37°C for the complexed form. The protein concentrations in various samples were 0.4–3.8 mM. For samples of protein–DNA complexes, the relative molar ratio of protein to DNA was determined by titration of DNA to protein while monitoring the upfield signals of methyl groups of the protein by ^1H NMR or by silver-stained native PAGE. Typically, the NMR samples of the complex were at a DNA/protein molar ratio of 1.4:1. Ratios of DNA to protein near or <1 resulted in greatly increased linewidths in the NMR spectra, making the samples unsuitable for NMR analyses.

All NMR spectra were acquired on a Bruker (Billerica, MA) model AMX 500 NMR spectrometer. For backbone assignments and the identification of secondary structural elements, the following NMR experiments were carried out: ^{15}N- and ^{13}C-resolved three-dimensional nuclear Overhauser effect spectroscopy/heteronuclear multiple-quantum correlation (NOESY-HMQC) (12) with a 60-msec mixing time, ^{15}N-resolved total correlated spectroscopy/heteronuclear single quantum correlation (TOCSY-HSQC) (13) with a 24-msec mixing time, and experiments correlating various nuclei of the peptide backbone including HNCA (14), HN(CO)CA (15), HNCO (14), and HACACO (16). (The latter experiments are named by the resonances that are observed.) In these experiments, carrier frequencies for ^1H, ^{15}N, $^{13}C^\alpha$, and ^{13}CO were 500.139, 50.684, 125.90, and 125.76 MHz, respectively. Typically 40, 32, 40, 80, and 1024 complex points were collected for ^{15}N, $^{13}C^\alpha$, ^{13}CO, indirectly detected ^1H, and observed ^1H dimensions, respectively. The sweepwidths used for the observed ^1H, indirectly detected ^1H, ^{15}N, $^{13}C^\alpha$, and ^{13}CO dimensions were 8333, 6250, 1299, 3774, and 2500 Hz, respectively, for the DNA-bound form, and 8333, 6250, 1524, 3019, and 1887 Hz, respectively, for the free form. In the ^{13}C-resolved NOESY-HMQC, a sweepwidth of 8772 Hz was used and 62 complex points were collected for the ^{13}C dimension. ^{15}N HSQC (17) spectra were collected with 128 complex points in the ^{15}N dimension. NMR data were processed and analyzed on Silicon Graphics (Mountain View, CA) computers using in-house written software (E.T.O. and R. Meadows, unpublished software). Linear prediction was employed to improve resolution in the indirect dimensions as described (18).

Amide exchange rates were measured from a series of ^{15}N HSQC spectra that were recorded for ≈3 hr each after the protein or protein–DNA complex sample in H_2O NMR buffer (see above) was exchanged into the ^2H_2O buffer.

For the free form, some of the NMR experiments were collected using samples of another version of Fli-1 containing residues 276–373 of Fli-1 and a 13-amino acid N-terminal vector leader sequence (MASMTGGQQMGRD). This protein [designated Fli-1-(276–373)L] bound specifically to DNA with essentially the same affinity as Fli-1-(276–373) (data not shown). When ^1H–^{15}N correlation (HSQC) (17) spectra of these two proteins were compared, there was essentially no difference between the amide proton and nitrogen chemical shifts for residues 280–373 (data not shown), indicating that chemical shift assignments of the two proteins can be used interchangeably for these residues.

RESULTS

Backbone Assignments. NMR structural studies were conducted on uniformly ^{15}N- or $^{15}N/^{13}C$-labeled Fli-1-(276–373) complexed with an unlabeled 16-bp DNA fragment containing a 9-bp consensus site for Fli-1 (9). The 16-bp long DNA site was used since shorter fragments of 14 and 12 bp resulted in reduced affinity to the protein (data not shown).

Sequential assignments of ^1H, ^{13}C, and ^{15}N resonances of the protein backbone were obtained by first identifying the resonances of adjacent residues by using two sets of heteronuclear three-dimensional NMR experiments. HNCA and HN(CO)CA experiments were used to correlate the amide proton and nitrogen resonances of residue i with the C^α chemical shifts of residues i and $i-1$. Ambiguities due to C^α degeneracy were resolved by using a second set of experiments that take advantage of the dispersion of carbonyl resonances. These experiments used an ^{15}N-resolved total correlated spectroscopy to correlate the amide proton and nitrogen signals to the H^α resonances of the same residue and a combination of HACACO and HNCO experiments to identify the H^α frequency of residue $i-1$. The adjacent spin systems identified from these two sets of experiments were further checked by nuclear Overhauser effects (NOEs) from ^{15}N-resolved NOESY spectra. To make sequential assignments, the spin systems had to be identified by amino acid type. Residue types were obtained unambiguously for >50% of the residues in the protein by using eight samples that were selectively ^{15}N-labeled by amino acid type. The amide proton and nitrogen resonances of Leu, Phe, Met, Lys, Arg, Tyr, Ile, and Gly/Ser were identified from HSQC experiments of these selectively labeled samples.

From these experiments, backbone assignments were obtained for 94% of the residues in Fli-1-(276–373) in the DNA-bound form. Assignments were not obtained for three amino acid residues (F362, G364, and Q367) near the C terminus. In addition, backbone assignments are also missing for N306-G307 and G353, which as will be shown are located in loops connecting strands in the β-sheet. The signals corresponding to these residues were weak, presumably caused by broad linewidths of the corresponding NMR signals.

Secondary Structure. A summary of the NMR data that define the secondary structure of the Fli-1 ets domain when bound to DNA is shown in Fig. 1. The secondary structural elements were identified from patterns of short- and medium-range NOEs (Fig. 1 *A–E*) that are characteristic of different types of secondary structures (19), deviations of $^1H^\alpha$, $^{13}C^\alpha$, and ^{13}CO chemical shifts (Fig. 1 *F–H*) from their random-coil values (20–22) and slow exchanging amide groups (Fig. 1*I*), which suggest their participation in the hydrogen-bonding network of α-helices or β-sheets.

As depicted in Figs. 1 and 2, the secondary structure of the Fli-1-(276–373) consists of three α-helices and a short four-stranded antiparallel β-sheet. The alignment of the β-strands was determined by interstrand NOEs obtained from three-dimensional ^{15}N- and ^{13}C-resolved NOESY spectra (Fig. 2). An α-helix (residues 284–294) is located near the N terminus followed by two β-strands. Residues 316–325 form a second helix followed by a loop leading to the third helix (residues

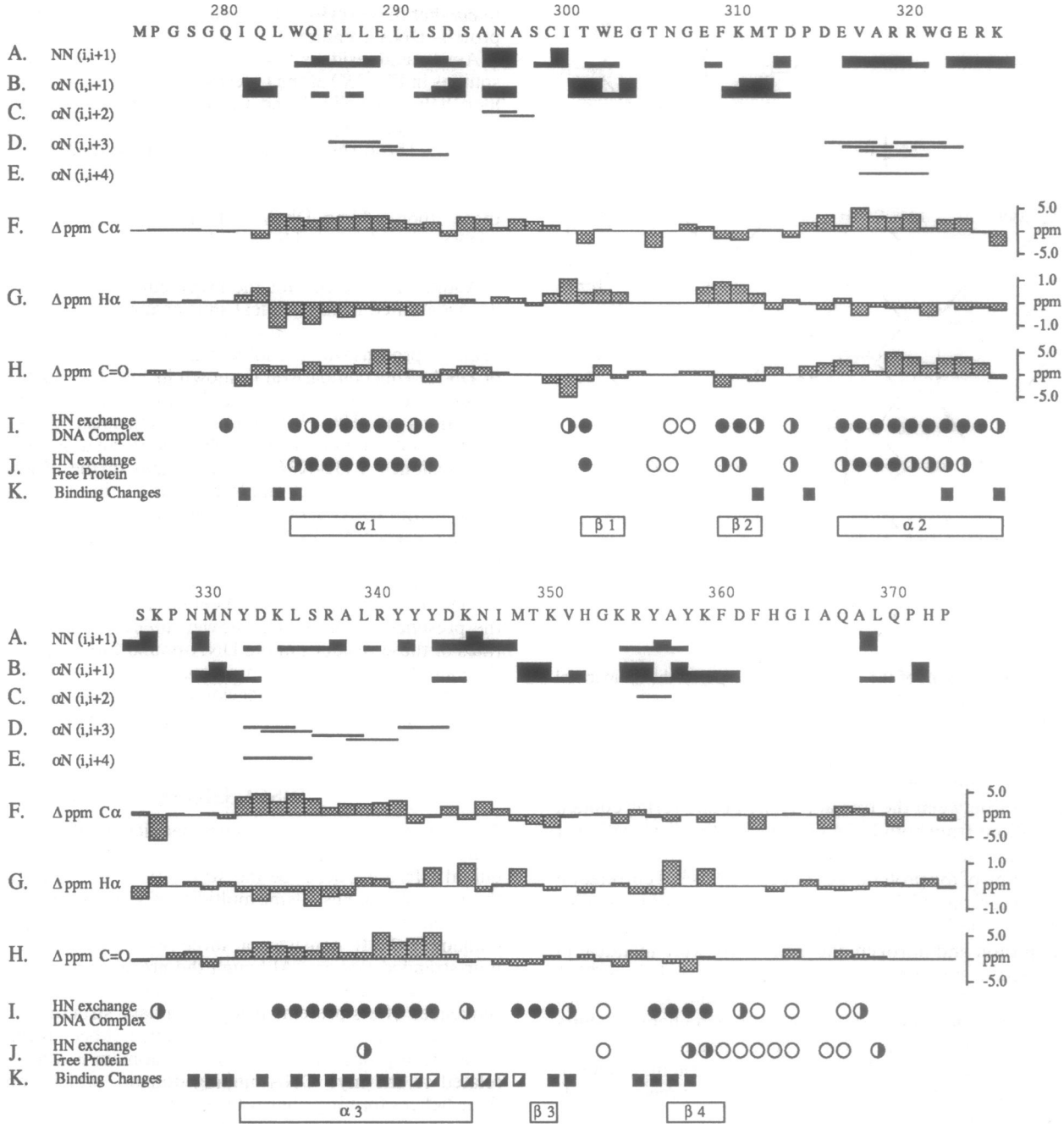

FIG. 1. Summary of NMR data used to identify the secondary structure of the Fli-1 ets domain in the DNA-bound form and residues influenced by DNA binding. The amino acid sequence of the Fli-1 ets domain and the residue number in full-length Fli-1 (8) are shown. NOEs between amide protons of consecutive residues (*A*) and between H^{α} and the amide proton of subsequent residues (*B–E*) are represented by bars connecting the residues. The thickness of the bar represents the intensity of the NOE. (*F–H*) Deviations of $^{13}C^{\alpha}$, $^{1}H^{\alpha}$, and ^{13}CO chemical shifts from random-coil values (20–22). (*I* and *J*) Amide proton exchange rates in the presence of DNA at 37°C (*I*) and in the absence of DNA at 25°C (*J*). Solid circles, slow exchange amides that were protected from exchange after 24 hr in $^{2}H_2O$; half-solid circles, intermediate exchange amides that were observed after 3 hr but not observed after 24 hr in $^{2}H_2O$; no circle, fast-exchange amides that were not observed after 3 hr in $^{2}H_2O$; open circles, residues for which HN and N assignments are not available. (*K*) Residues whose chemical shifts of backbone resonances are strongly affected by DNA binding. Residues with large (see below) chemical shift changes in any of the five backbone resonances (^{15}N, ^{1}HN, $^{13}C^{\alpha}$, $^{1}H^{\alpha}$, or ^{13}CO) between the free and DNA-bound forms and not involved in dimerization are represented by solid squares. Residues with large chemical shift changes but also involved in dimerization are represented by half-solid squares. The chemical shift change was considered large if it was greater in magnitude than 1.43, 0.81, 0.36, 0.35, or 0.87 ppm for ^{15}N, ^{1}HN, $^{13}C^{\alpha}$, $^{1}H^{\alpha}$, or ^{13}CO, respectively. These cutoff values were the sum of the mean and standard deviation of the chemical shift changes for all residues. Secondary structures derived from NMR analyses are indicated at the bottom.

332–345). At the C terminus, two more β-strands pair with the first two strands to form a four-stranded antiparallel β-sheet.

DNA Binding. To identify regions in the Fli-1 ets domain that are involved in DNA binding, we obtained backbone assignments for the protein in the free form and compared these chemical shifts to those of the protein when bound to DNA. However, this comparison is complicated by the fact that at the concentration needed to carry out the NMR experiments, the protein forms a dimer in the absence of DNA, as determined by analytical sedimentation and dynamic light scattering analyses (J. Harlan and E. Matayoshi, personal communication). In the presence of DNA, the

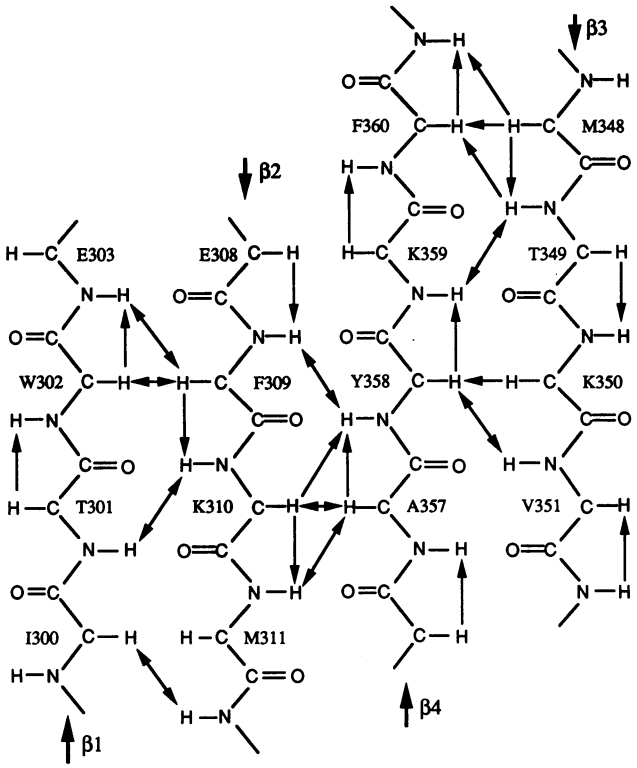

FIG. 2. Alignment of the four strands (β1–β4) in the antiparallel β-sheet of the Fli-1 ets domain. Arrows indicate observed sequential and interstrand NOEs.

protein dimer is disrupted and the protein–DNA complex exists in a monomeric form. Therefore, the chemical shift differences between the free and DNA-bound forms contain contributions from both DNA binding and the dissociation of the protein dimer. To identify residues involved in the dimerization of the protein, we collected a ^{1}H–^{15}N correlation (HSQC) spectrum of the free form at a concentration (50 μM) where the protein is predominantly monomeric. Most of the amide proton and nitrogen chemical shifts were identical in the monomer and dimer. However, in three regions of Fli-1 (amino acids W302–E308, Y342–M348, and L369–Q370), differences in the amide proton and nitrogen chemical shifts were observed (data not shown), suggesting that these residues are involved in the dimerization of the protein. Chemical shift changes in the presence of DNA in other regions must, therefore, be due to DNA binding.

Fig. 1*K* summarizes the comparisons of chemical shifts of five backbone resonances (^{15}N, ^{1}HN, $^{13}C^{\alpha}$, $^{1}H^{\alpha}$, or ^{13}CO) of the Fli-1 ets domain in the free and DNA-bound forms and shows the residues that are most strongly affected by the presence of DNA. Residues with large differences in chemical shift between the free and DNA-bound forms but no differences between the monomer and the dimer are mainly located in the C-terminal half of the protein and include the third helix, the loop leading to this helix, the third and fourth strands of the β-sheet, and the loop connecting these two strands. In addition to these residues, large backbone chemical shift differences were also observed in three residues near the beginning of the first helix and in several residues of the second β-sheet strand, the second helix, and the loop between them. This suggests that these regions either directly interact with DNA or undergo a conformational change upon DNA binding. The secondary structure of the Fli-1 ets domain in the absence of DNA (data not shown) is essentially the same as the DNA-bound form, suggesting that there are no gross structural changes upon DNA binding. Thus, it is likely that these regions are in close proximity to DNA in the protein–DNA complex.

Amino acid residues Y342–M348 (represented by half-solid squares in Fig. 1*K*) at the C-terminal end of helix 3 and in the loop between helix 3 and the third strand of the β-sheet showed large changes of backbone chemical shifts upon DNA binding. These residues are also involved in dimerization. The magnitudes of changes of amide proton and nitrogen chemical shifts from dimer to monomer are much less than those upon adding DNA (data not shown). It therefore appears that these residues could also be affected by DNA binding.

Additional evidence for the involvement of the Fli-1 residues identified from chemical shift changes in DNA binding is obtained from the differences in rates of chemical exchange of amide protons with the solvent in the presence and absence of DNA. This comparison is shown in Fig. 1 *I* and *J*. In the absence of DNA, sequential and medium-range NOEs and deviations of $^{1}H^{\alpha}$, $^{13}C^{\alpha}$, and ^{13}CO chemical shifts from random coil values indicate a helical conformation for amino acid residues Y332–K345. At 25°C and in the absence of DNA, the half-lives of amide protons of these residues in helix 3 (with the exception of L339) are <2 hr. At 37°C and in the presence of DNA, the half-lives of amide protons of residues in the third helix are >24 hr. The exchange rates of several residues surrounding this helix at the end of the second helix and the third β-sheet strand are also slowed in the presence of DNA. The slower amide proton exchange rates of these residues in the DNA-bound form indicate that their amide groups become protected from the solvent by the presence of DNA. This suggests that the residues in these regions are involved in contacting DNA in the protein–DNA complex.

DISCUSSIONS

To understand the DNA-binding specificities of the ets proteins at the molecular level, structural information is required. Here we describe the structural characterization of this class of proteins. Using multidimensional NMR, we have determined the secondary structure of the ets domain of human Fli-1. It consists of three α-helices and a short four-stranded β-sheet. Although the presence and locations of the helices have been correctly predicted from the primary sequences of ets proteins using secondary structure prediction algorithms (5, 6), the β-strands have not been identified. It has been proposed (7) that the ets domain is structurally related to the myb DNA-binding domain, which contains three helices forming a helix–turn–helix-like structure similar to those of the cro repressor of bacteriophage 434 and the homeodomain (23). However, our results show that the overall secondary structures of the ets domain of Fli-1 and myb are not similar.

By comparing chemical shifts and amide proton exchange rates of the protein free in solution and complexed to DNA, we found that residues in helix 3 are strongly affected by DNA binding. This agrees with the available mutagenesis data on the DNA binding of ets domains (5, 6, 24). Bosselut *et al.* (5) showed that a single amino acid substitution in Ets-1, at a position equivalent to K334 of Fli-1 in the third helix, was able to change the DNA-binding specificity of Ets-1 to that of Elf-1. As has been noticed by others (5, 6), this helix is amphipathic with polar and charged residues on one side that could interact with DNA as the recognition helix and hydrophobic residues on the opposite side that could dock the helix to the protein core. On the basis of common features of recognition helices of eukaryotic DNA-binding proteins, Suzuki (25) predicted that helix 2 corresponds to the recognition helix in ets proteins. However, the sequence of helix 3 also aligns well with those of recognition helices in other

eukaryotic DNA-binding proteins, and our NMR results and published mutagenesis data (5) suggest that helix 3 of the Fli-1 ets domain is the recognition helix.

The secondary structure of the Fli-1 ets domain determined by our NMR studies resembles that of the DNA-binding domain of catabolite gene activator protein (CAP) from *E. coli* (26). The two proteins have a primary sequence homology of 20% over 80 aligned residues (Fig. 3). CAP belongs to the family of helix–turn–helix prokaryotic DNA-binding proteins (27). Several eukaryotic proteins including the globular domain of the linker histone H5 (28), the HNF-3/fork head family (29), and the heat shock transcription factor (30, 31) are known to be structurally similar to CAP. The DNA-binding domains of these proteins all have three helices and a short antiparallel β-sheet composed of three or four strands. In addition to having similar secondary structures, like other members of this structural family, the ets domain also utilizes the third helix as the principal element for DNA recognition. Additional contacts of the Fli-1 ets domain with the DNA suggested by the NMR data include residues in the loop connecting the third and fourth β-strand, and near the N terminus of the first helix. These data are also consistent with the structures of DNA complexes of CAP and HNF-3γ, where similar contacts were observed (26, 29). Thus, it appears that the ets domain does not constitute a distinct structural motif for DNA binding, as previously thought (2), but resembles the CAP family of helix–turn–helix proteins.

Although a detailed structural comparison awaits a high-resolution structure of the ets domain, some obvious differences between the ets domain and the well-characterized proteins with similar folds can already be identified. Compared to CAP, the tight turn in the helix–turn–helix motif of CAP is lengthened to a loop in the Fli-1 ets domain, as in other eukaryotic DNA-binding proteins in this family. The HNF-3/fork head motif has been referred to as a "winged helix" (29) in which the recognition helix is flanked by a loop connecting the last two β-strands on one side and a long loop at the C terminus on the other side. Both of these loops interact with DNA, in addition to the recognition helix. The ets domain does not appear to have the second wing formed by the C-terminal loop, as residues beyond the last strand of the β-sheet can be deleted without abolishing DNA binding (32). These differences and the structural resemblance of the ets protein to CAP and related proteins remain to be elucidated by the determination of the complete tertiary structure of the protein and protein–DNA complex.

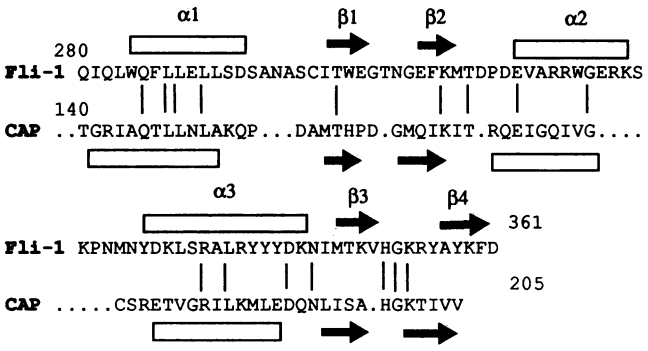

FIG. 3. Sequence and secondary structure alignment of the Fli-1 ets domain to CAP DNA-binding domain. The sequences of the Fli-1 ets domain and CAP were aligned by first superimposing the secondary structures of the two proteins. The two sequences were adjusted relative to each other by matching the homologous residues (indicated by vertical lines) of the two proteins. The amino acid sequence and the secondary structure for CAP were from ref. 26. Secondary structures are drawn schematically, where boxes represent α-helices and arrows represent β-strands.

We thank J. Harlan and E. Matayoshi for ultracentrifugation and light scattering analyses, R. Xu for assisting in NMR experiments, B. Petryniak for initial protein purification, J. Leiden and H. Singh for helpful discussions, and T. Logan and A. Petros for critically reading the manuscript. The research in The University of Chicago was supported by Howard Hughes Medical Institute.

1. Wasylyk, B., Hahn, S. L. & Giovane, A. (1993) *Eur. J. Biochem.* **211**, 7–18.
2. Karim, F. D., Urness, L. D., Thummel, C. S., Klemsz, M. J., McKercher, S. R., Celada, A., Van Beveren, C., Maki, R. A., Gunther, C. V., Nye, J. A. & Graves, B. J. (1990) *Genes Dev.* **4**, 1451–1453.
3. Anton, I. A. & Frampton, J. (1988) *Nature (London)* **336**, 719.
4. Nye, J. A., Petersen, J. M., Gunther, C. V., Jonsen, M. D. & Graves, B. J. (1992) *Genes Dev.* **6**, 975–990.
5. Bosselut, R., Levin, J., Adjadj, E. & Ghysdael, J. (1993) *Nucleic Acids Res.* **21**, 5184–5191.
6. Mavrothalassitis, G., Fisher, R. J., Smyth, F., Watson, D. K. & Papas, T. S. (1994) *Oncogene* **9**, 425–435.
7. Laget, M.-P., Callebaut, I., de Launoit, Y., Stehelin, D. & Mornon, J.-P. (1993) *Nucleic Acids Res.* **21**, 5987–5996.
8. Delattre, O., Zucman, J., Plougastel, B., Desmaze, C., Melot, T., Peter, M., Kovar, H., Joubert, I., de Jong, P., Rouleau, G., Aurias, A. & Thomas, G. (1992) *Nature (London)* **359**, 162–165.
9. Mao, X., Miesfeldt, S., Yang, H., Leiden, J. M. & Thompson, C. B. (1994) *J. Biol. Chem.* **269**, 18216–18222.
10. Sambrook, J., Fritsch, E. F. & Maniatis, T. (1989) *Molecular Cloning: A Laboratory Manual* (Cold Spring Harbor Lab. Press, Plainview, NY), 2nd Ed.
11. Hoffman, D. W. & Spicer, L. D. (1991) *Techniques in Protein Chemistry* (Academic, San Diego), Vol. 2, pp. 409–416.
12. Fesik, S. W. & Zuiderweg, E. R. P. (1988) *J. Magn. Reson.* **87**, 588–593.
13. Marion, D., Kay, L. E., Sparks, S. W., Torchia, D. A. & Bax, A. (1989) *J. Am. Chem. Soc.* **111**, 1515–1517.
14. Kay, L. E., Ikura, M., Tschudin, R. & Bax, A. (1990) *J. Magn. Reson.* **89**, 496–514.
15. Bax, A. & Ikura, M. (1991) *J. Biomol. NMR* **1**, 99–104.
16. Grzesiek, S. & Bax, A. (1993) *J. Magn. Reson. Ser. B* **102**, 103–106.
17. Bodenhausen, G. & Ruben, D. J. (1980) *J. Chem. Phys. Lett.* **69**, 185–189.
18. Olejniczak, E. T. & Eaton, H. L. (1990) *J. Magn. Reson.* **87**, 628–632.
19. Wüthrich, K. (1986) *NMR of Proteins and Nucleic Acids* (Wiley, New York).
20. Spera, S. & Bax, A. (1991) *J. Am. Chem. Soc.* **113**, 5490–5492.
21. Wishart, D. S., Sykes, B. D. & Richards, F. M. (1992) *Biochemistry* **31**, 1647–1651.
22. Richarz, R. & Wüthrich, K. (1978) *Biopolymers* **17**, 2133–2141.
23. Ogata, K., Hojo, H., Aimoto, S., Nakai, T., Nakamura, H., Sarai, A., Ishii, S. & Nishimura, Y. (1992) *Proc. Natl. Acad. Sci. USA* **89**, 6428–6432.
24. Wang, C.-Y., Petryniak, B., Ho, I.-C., Thompson, C. B. & Leiden, J. M. (1992) *J. Exp. Med.* **75**, 1391–1399.
25. Suzuki, M. (1993) *EMBO J.* **12**, 3221–3226.
26. Schultz, S. C., Shields, G. C. & Steitz, T. A. (1991) *Science* **253**, 1001–1007.
27. Pabo, C. O. & Sauer, R. T. (1992) *Annu. Rev. Biochem.* **61**, 1053–1095.
28. Ramakrishnan, V., Finch, J. T., Graziano, V., Lee, P. L. & Sweet, R. M. (1993) *Nature (London)* **362**, 219–223.
29. Clark, K. L., Halay, E. D., Lai, E. & Burley, S. K. (1993) *Nature (London)* **364**, 412–420.
30. Harrison, C. J., Bohm, A. A. & Nelson, H. C. M. (1994) *Science* **263**, 224–227.
31. Vuister, G. W., Kim, S.-J., Wu, C. & Bax, A. (1994) *Biochemistry* **33**, 10–16.
32. Janknecht, R. & Nordheim, A. (1992) *Nucleic Acids Res.* **20**, 3317–3324.